Analyzing and Modeling the Spread of SARS-CoV-2 Omicron Lineages BA.1 and BA.2, France, September 2021–February 2022

Mircea T. Sofonea, Bénédicte Roquebert, Vincent Foulongne, David Morquin, Laura Verdurme, Sabine Trombert-Paolantoni, Mathilde Roussel, Jean-Christophe Bonetti, Judith Zerah, Stéphanie Haim-Boukobza, Samuel Alizon

We analyzed 324,734 SARS-CoV-2 variant screening tests from France enriched with 16,973 whole-genome sequences sampled during September 1, 2021–February 28, 2022. Results showed the estimated growth advantage of the Omicron variant over the Delta variant to be 105% (95% CI 96%–114%) and that of the BA.2 lineage over the BA.1 lineage to be 49% (95% CI 44%–52%). Quantitative PCR cycle threshold values were consistent with an increased ability of Omicron to generate breakthrough infections. Epidemiologic modeling shows that, in spite of its decreased virulence, the Omicron variant can generate important critical COVID-19 activity in hospitals in France. The magnitude of the BA.2 wave in hospitals depends on the level of relaxing of control measures but remains lower than that of BA.1 in median scenarios.

The Omicron SARS-CoV-2 variant of concern (Pango lineage B.1.1.529, GISAID clade GR/484A) was detected in South Africa on November 26, 2021 (*1*). Rapid analyses demonstrated its increased transmissibility (C.A.B. Pearson et al., unpub. data, https://doi.org/10.1101/2021.12.19.21268038), high immune evasion potential (*2*,*3*), and low virulence (*4*–*6*) compared with the Delta variant. Furthermore, the biology of the virus appears to be different, having the potential to enter human cells through endocytosis and a pronounced tropism for the upper respiratory tract (*7*–*9*; T.P. Peacock et al., unpub. data, https://doi.org/10.1101/2021.12.31.474653; B.J. Willett et al., unpub. data, https://doi.org/10.1101/2022.01.03.21268111). After South Africa, the Omicron variant caused epidemic waves in many countries, including the United Kingdom (*10*), Denmark (*11*), and countries of North America (*12*).

The first Omicron lineage to dominate was BA.1 (B.1.1.529.1, Nextstrain clade 21K). However, in some countries, such as Denmark, its sister lineage BA.2 (former B.1.1.529.2, Nextstrain clade 21L) rapidly became dominant. BA.1 and BA.2 are highly divergent lineages (A.Z. Mykytyn et al., unpub. data, https://doi.org/10.1101/2022.02.23.481644), but their virulence and biology appear to be similar and the cross-immunity strong (M. Stegger et al., unpub. data, https://doi.org/10.1101/2022.02.19.22271112). Early reports suggest that BA.2 has a growth advantage over BA.1 (F.P. Lyngse et al., unpub. data, https://doi.org/10.1101/2022.01.28.22270044), possibly from a shorter generation time (i.e., average delay between consecutive infections in a transmission chain) (*10*).

Since January 2021, all the positive samples in France have been screened with variant-specific quantitative PCR (qPCR) assays targeting specific mutations (*13*). This close monitoring of the epidemic has low specificity, and the mutations targeted need to be updated to match the circulating variants, which is also why the monitoring is complemented by the whole-genome sequencing (WGS) of a subset of the samples.

We analyzed 324,734 variant-specific screening tests performed during September 1, 2021–February 28, 2022, in all 13 regions of mainland France. To understand lineage circulation, we generated SARS-CoV-2 whole-genome sequences for 16,973 of

Author affiliations: Université de Montpellier, Montpellier, France (M.T. Sofonea); Laboratoire Cerba, Saint Ouen L'Aumône, France (B. Roquebert, L. Verdurme, S. Trombert-Paolantoni, M. Roussel, S. Haim-Boukobza); Centre Hospitalier Universitaire de Montpellier, Montpellier (V. Foulongne, D. Morquin); Laboratoire Cerballiance Paris et Île-de-France Est, Paris, France (J.-C. Bonetti, J. Zerah); Centre National de la Recherche Scientifique, Paris (S. Alizon)

DOI: https://doi.org/10.3201/eid2807.220033

Table 1. Main characteristics of SARS-CoV-2 variant-specific screening tests (N = 131,478), France, September 1–December 18, 2021*

Characteristic	Value
Age of patient, y, median (95% CI)	36 (6–74)
Assay	
TIB Molbiol	4,887 (3.7)
PerkinElmer	33,037 (25.1)
ID Solutions (Evolution)	93,554 (71.2)
Context	
General population	127,337 (96.9)
Hospital	4,141 (3.1)
Region	
Ile-de-France	51,407 (39.1)
Hauts-de-France	16,938 (12.9)
Normandie	11,996 (9.1)
Nouvelle-Aquitaine	8,516 (6.5)
Provence-Alpes-Côte d'Azur	7,549 (5.7)
Occitanie	7,143 (5.4)
Corse	5,528 (4.2)
Bourgogne-Franche-Comté	5,155 (3.9)
Grand Est	5,136 (3.9)
Centre-Val de Loire	4,811 (3.7)
Bretagne	3,455 (2.6)
Other	1,296 (0.9)
Outcome	
A0B0C1	101,970 (77.6)
A0B0C0	6,969 (5.3)
A0B1C1	899 (0.68)
A1B0C1	37 (<0.1)
A1B0C0	15 (<0.1)
Other	21,588 (16.4)

*Values are no. (%) patients except as indicated.

these samples (5.2%) over the same period. We analyzed the cycle threshold (Ct) values of the qPCR to gain further insights into the biology and epidemiology of the infections. Finally, we used these results to explore prospective scenarios regarding the dynamics of critical care unit (CCU) occupancy in France in 2022. This study was approved by the Institutional Review Board of the Centre Hospitalier Universitaire of Montpellier and is registered at ClinicalTrials.gov (identifier no. NCT04738331).

Table 2. Results of ID Solution Revolution SARS-CoV-2 variant-specific screening tests (N = 193,256), France, December 18, 2021–February 28, 2022*

Characteristic	Value
Age of patient, y, median (95% CI)	36 (6–74)
Context	
General population	187,292 (96.9)
Hospital	5,964 (3.1)
Region	
Ile-de-France	40,185 (20.8)
Hauts-de-France	26,382 (13.7)
Normandie	31,205 (16.2)
Nouvelle-Aquitaine	13,236 (6.9)
Provence-Alpes-Côte d'Azur	31,299 (16.2)
Occitanie	9,034 (4.7)
Corse	8,031 (4.2)
Bourgogne-Franche-Comté	4,366 (2.3)
Grand Est	6,865 (3.6)
Centre-Val de Loire	10,412 (5.4)
Bretagne	9,405 (4.9)
Other	2,836 (1.5)
Outcome	
A0B9C1D0	12,955 (6.7)
A0B9C0D1	154,134 (79.8)
A0B9C1D1	173 (0.1)
A1B9C0D0	4,762 (2.5)
Other	21,232 (10.9)

*Values are no. (%) patients except as indicated.

Methods

Cohort Description

The variant screening tests were performed by Cerba Laboratory (Saint Ouen L'Aumône, France) on samples that originated from partner centers in mainland France and tested positive for SARS-CoV-2 with a generic qPCR assay. Most of the samples originated from the general population (Tables 1, 2). We did not have access to additional details about patient symptoms; however, according to an earlier study on a similar cohort, nearly all the samples originated from nasopharyngeal swab specimens, and the proportion of symptomatic and asymptomatic individuals were comparable among the positive tests (*14*). To limit epidemiologic biases, we removed persons >80 years or <5 years of age from the dataset.

Variant-Specific Screening Tests

We first analyzed 131,478 screening tests performed during September 1–December 18, 2021. The assays used over this first period were ID SARS-CoV-2/VOC Evolution Pentaplex (ID Solutions, https://www.id-solutions.fr) (93,554 tests), VariantDetect (PerkinElmer, https://www.perkinelmer.com) (33,037 tests), and VirSNiP (TIB Molbiol, https://www.tib-molbiol.de) (4,887 tests). These tests targeted 3 mutations in the SARS-CoV-2 spike protein: E484K (mutation A), E484Q (mutation B), and L452R (mutation C). Denoting the absence of a mutation by a 0 and its presence by 1, A0B0C1 mostly corresponds to infections caused by the Delta variant, A0B0C0 to the Alpha or Omicron variant or an ancestral lineage, A0B1C1 to Kappa or Kappa-like variants, A1B0C0 to the Beta or the Gamma variant, and A1B0C1 to a Delta variant with an E484K mutation.

Because of the shift in variant frequencies, new screening assays were implemented in late 2021. We analyzed 193,256 tests performed during December 6, 2021–February 28, 2022, all using the assay ID SARS-CoV-2/VOC Revolution Pentaplex (ID Solutions). This assay still targeted mutations A and mutation C but also targeted S:K417N (mutation D). Denoting nontested mutations with a 9, then A0B9C1D0 most likely indicates infections caused by the Delta variant, A0B9C0D1 by the Omicron

variant, A1B9C0D0 by the Gamma variant, A1B9C0D1 by the Beta variant, and A0B9C0D0 by the Alpha variant or the B.1.640 lineage. Finally, A0B9C1D1 can either indicate an infection by Delta with a 417N mutation, Omicron with a 452R mutation, or a Delta–Omicron co-infection.

For the ID Solutions Pentaplex tests, we analyzed 4 Ct values. Three of these values correspond to primers targeting the mutations of interest: S:417N, S:452R, or S:484K, the last to a primer targeting the nucleoprotein gene, which was used as a control.

Whole-Genome Sequencing

Next-generation sequencing (NGS) was performed by Cerba Laboratory for 16,973 samples with a Ct <30 using the CovidSeq amplicon-based NGS assay according to supplier recommendations (Illumina, https://www.illumina.com) and after a Janus/Chemagic RNA extraction (Perkin Elmer) from the nasopharyngeal swab. All sequences obtained were submitted to the EMERGEN Consortium Database (Santé Publique France, https://www.santepubliquefrance.fr/dossiers/coronavirus-covid-19/consortium-emergen) and GISAID (https://www.gisaid.org).

Statistical Analyses

Multinomial log-Linear Model

We performed a multinomial log-linear model with the formula variant = $\beta_0 + \beta_1$ age + β_2 assay + β_3 location_sampling + β_4 date:region + ε, where the β_i are the model parameters, ε the residuals, and the variable age is the individual age (treated as an integer and centered and scaled), location_sampling is a binary variable indicating whether the sample was collected in a hospital or in the general population, assay is the qPCR assay used, date is the sampling date (treated as an integer and centered and scaled), and region is the administrative region of residency in France. We included interactions between region and sampling date to detect temporal trends.

To make results easier to interpret, we computed relative risk ratios (RRRs). These ratios reflect, for a given variable, the risk for belonging to 1 of the outcomes (variant detection in this study) compared with the control group.

Growth Advantage Calculation

We computed growth advantages by using earlier methods based on Malthusian population growth rates (*15*–*18*). If we denote by $p(t)$ the frequency of an allele of interest (e.g., A0B0C0 test results) in the population (e.g., A0B0C0 and A0B0C1 test result), then the selection coefficient corresponds to the following rate:

$$s = \frac{\mathrm{d}}{\mathrm{d}t} \log\left(\frac{p(t)}{1-p(t)}\right).$$

This value is the inverse of a duration, and comparing it to earlier estimates requires a scaling for the generation time, the mean of which, T, is approximated by the mean serial interval (*19*). Overall, the growth advantage of a variant (e.g., A0B0C0) over another (e.g., A0B0C1) scaled for 1 infection generation is denoted as s_T and given by the formula $s_T = s \times T$. We estimated s_T by using the fitted values from a generalized linear model with a logit link to control for the covariates listed.

We used 21-day windows to estimate growth advantage, which corresponds to >4 generations of infection given the average generation time used. This number was chosen to be able to detect potential signals, while still obtaining a good temporal resolution of the estimated.

Ct Values Linear Modeling

We used a linear model with the following formula: Ct = $\gamma_0 + \gamma_1$ age + γ_2 variant + γ_3 location_sampling + γ_4 date × region + ε, where the γ_i indicate the model parameters, ε the residuals, and the covariates are the same as in the multinomial model. The variant was determined either by reverse transcription qPCR or WGS. The sampling date was included in the model because growing epidemics can be associated with lower Ct values than declining epidemics (*14*,*20*).

Using a likelihood ratio test, we showed that the presence of the variant covariate does improve the model. We assessed covariate significance by using an analysis of variance (ANOVA) with a type II error using the ANOVA function from the companion to applied regression package in R (R Project for Statistical Computing, https://www.r-project.org). We computed estimated marginal means for the Ct values associated with the screening tests results by using the emmeans function from the eponym R package. We plotted the fitted values from the linear model by using the predict function in R. The statistical methods are further described (Appendix 1, https://wwwnc.cdc.gov/EID/article/28/7/22-0033-App1.pdf), and raw data and R scripts are available online (https://doi.org/10.5281/zenodo.6536220).

Epidemiologic Modeling

We used the previously developed framework Covidsim, which accurately captures the national CCU admissions for SARS-CoV-2 in France and the associated

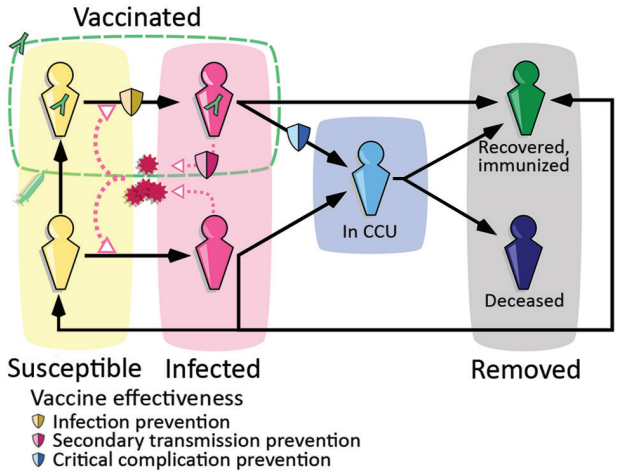

Figure 1. Epidemiologic modeling of the SARS-CoV-2 Omicron BA.2 wave dynamics, France. Simplified flowchart of the Covidsim framework. Persons can move between several compartments in the general population (in yellow or pink depending on the infection status), in CCUs in blue and removed from the system, either because of their immunity to BA.2 or of death (in gray). Part of the general population is vaccinated (green dashed line), which affects epidemiologic dynamics in 3 ways (illustrated with the shields), namely reduced infectivity, reduced virulence, and reduced risk for infection. CCU, critical care unit.

mortality incidence time series (*21*). The underlying model is deterministic, is structured in discrete time, and uses CCU incidence and prevalence data, as well as mortality data, to estimate parameters of interest (Figure 1, Appendix 1). A retrospective analysis showed its ability to provide robust projections up to 5 weeks ahead (*22*).

In the model, the number of vaccinated persons followed the national campaign in France (Système d'Information VAccin Covid data) and the number of persons with postinfectious immunity results from the model's reconstruction of the epidemic. The protection against infection and severe illness depends on the type of immunity (vaccine [*23*] or postinfectious [*24*]) and the variant. These values, like others, were informed from literature data, technical reports, and preliminary work.

Having a mechanistic model enables us to explore prospective scenarios for CCU activity. We did so by formulating assumptions regarding the intensity of future control measures and incorporating our estimates of growth advantage and relative frequency of the variants into the model.

In this study, the temporal reproduction number (Rt) corresponds to the average number of secondary infections caused by an infected person at date t and is estimated by using national hospital admission data (https://www.data.gouv.fr/fr/datasets/donnees-hospitalieres-relatives-a-lepidemie-de-covid-19) and the EpiEstim method (*25*). We shifted the dates in the incidence time series to compute Rt, setting the median time between infection and CCU admission to 14 days (*21*,*26*).

Results

A0B0C0 Emergence

We first analyzed variant-specific screening tests collected during September 1–December 18, 2021 (Figure 2, panel A). Most of these tests originated from the general population (96.6%) and showed coverage differences between regions of France (Table 1). The most common assay used (71%) was that from ID

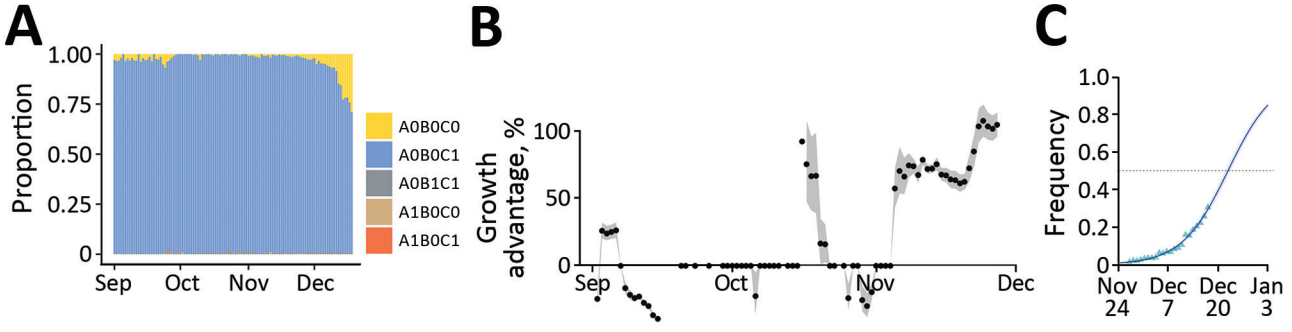

Figure 2. Monitoring and quantifying variant spread in using SARS-CoV-2 variant-specific screening tests (N = 103,757), France, October 1–December 18, 2021. A) Raw proportion of the test outcomes. B) Growth advantage of A0B0C0 tests over A0B0C1 in France. Points indicate the median growth advantage estimated on a 21-day sliding window; the gray shading indicates 95% CI. C) Estimated frequency and growth advantage of A0B0C0 relative to the sum of A0B0C0 and A0B0C1 tests in France, corresponding to the last point of panel A. Triangles show the fitted values from the model, the line the model output, and the gray shading the 95% CI. Raw occurrence data from panel A is stratified by region in Appendix 1 Figure 1 (https://wwwnc.cdc.gov/EID/article/28/7/22-0033-App1.pdf). Test designations indicate the absence of a mutation by a 0 and its presence by 1; the mutations are S:484K (A), S:E484Q (B), and S:452R (C); A0B0C1 mostly corresponds to Delta variant, A0B0C0 to Alpha or Omicron variant or an ancestral lineage, A0B1C1 to Kappa or Kappa-like variants, A1B0C0 to Beta or the Gamma variant, and A1B0C1 to a Delta variant with an E484K mutation.

Solutions (Evolution). The raw number of tests performed follows the incidence curve of the epidemic (Appendix 1 Figure 1).

Focusing on the tests performed during October 25–December 18, 2021 (i.e., when the epidemic was increasing), we used a multinomial regression model to identify covariates associated with the test outcome (Table 3). A0B0C0 infections (consistent with Omicron) were found in younger persons than were A0B0C1 infections (consistent with Delta); RRR was 0.85 (95% CI 0.83–0.88) per age unit (equal to 56 years in this study). We also detected strong temporal increases in most of the regions of France that had RRR >10 per day. In some regions, we detected a temporal increase of A0B1C1 tests, consistent with the Kappa variant. Finally, in our dataset, the (rare) A1B0C1 tests only showed a slight temporal increase in 2 regions (Bretagne and Hauts-de-France).

We then estimated growth advantages of A0B0C0 over A0B0C1 infections during 21-day time windows. The advantage was adjusted for covariates and assumed to be constant over each window. In September 2021, A0B0C0 infections were spreading less rapidly than A0B0C1 (Figure 2, panel B). This finding is consistent with the rapid increase of the Delta variant at the time (*18*). The pattern shifted at the end of November, with a 50% growth advantage of A0B0C0 infections, which increased to 105% (95% CI 96.1%–114%) in the last time window. According to this model, A0B0C0 infections became more frequent than A0B0C1 infections during the week of December 20 (Figure 2, panel C), with strong variations across regions (Appendix 1 Figure 1).

The A0B9C0D1/Omicron Wave

The new screening test targeting the K417N mutation enabled us to better document the spread of the Omicron variant (Table 2). In December 2021, the A0B0C0 wave was mainly caused by viruses bearing the K417N mutation (Figure 3, panel A). Furthermore, the proportion of A0B0C0 tests not attributable to Omicron decreased toward the end of the year. Finally, we also noted potential co-infections of Omicron and Delta in December.

We then estimated the growth advantage of A0B9C0D1 over A0B9C1D0 during December 6, 2021–February 28, 2022 (Figure 3, panel B). The resulting estimate (96.5% [95% CI 87.9%–105%]) is very consistent with the results obtained using a less-specific test on the early stages of the wave.

We observed a shift between the Omicron waves in the different regions of France (Figure 4). For instance, in the South-East area, Delta was still dominant during week 51 of 2021. As expected, we also saw that tests consistent with co-infections of Omicron and Delta were more frequent in regions where the 2 variants were cocirculating in substantial

Table 3. Relative risk ratios of covariates associated with SARS-CoV-2 variant-specific screening tests (N = 103,757), France, October 1–December 18, 2021*

Covariate	Relative risk ratio (95% CI)				
	A0B0C0	A0B1C1	A1B0C0	A1B0C1	Other
Intercept	0 (0.00–0.01)	0.01 (0–01)	NS (0–0)	NS (0–0)	0.18 (0.17–0.18)
Age, scaled†	0.85 (0.83–0.88)	1.08 (1.0–1.2)	NS (0.7–2.4)	NS (0.5–1)	0.82 (0.8–0.83)
Context					
General population	Referent	Referent	Referent	Referent	Referent
Hospital	NS (0.82–1.1)	0.37 (0.2–0.69)	NS —	NS —	0.88 (0.79–0.99)
Assay					
ID Solutions	Referent	Referent	Referent	Referent	Referent
PerkinElmer	2.0 (1.8–2.1)	0.46 (0.38–0.56)	NS (0–3.8)	NS (0.1–1.1)	0.82 (078–0.85)
TIB Molbiol	2.1 (1.6–2.6)	10.9 (9–13)	NS (0.9–23)	8.3 (3.1–22)	1.94 (1.8–2.1)
Date and region					
Ile-de-France	87.0 (75–100)	4.4 (3.4–5.7)	NS (0–7.5)	NS (0.3–6.5)	1.7 (1.6–1.8)
Bourgogne-Franche-Comté	10.5 (7.8–14)	8.3 (5.6–12)	NS (no values)	NS (0–49)	0.63 (0.53–0.74)
Bretagne	37.6 (28–51)	NS (0.91–5.4)	NS (no values)	21.6 (2–200)	1.3 (1.1–1.6)
Centre-Val de Loire	46.1 (37–57)	NA (0.8–3.5)	NS (0–370)	NS (0–98)	NS (0–0)
Corse	86.4 (71–100)	0.2 (0.05–0.5)	NS (0–310)	NS (0–56)	1.9 (1.7–2.2)
Grand Est	22.2 (18–28)	3.7 (2.3–5.8)	NS (0.5–80)	NS (0–100)	0.49 (0.42–0.58)
Hauts-de-France	44.8 (38–53)	NS (0.4–1.2)	NS (0–10)	18.0 (5.5–58)	1.17 (1.10–1.30)
Normandie	38.2 (32–46)	2.2 (1.4–3.4)	NS (0–23)	NS (0–15)	0.77 (0.69–0.86)
Nouvelle-Aquitaine	17.6 (14–22)	2.7 (1.7–4.4)	NS (0–51)	NS (0–16)	0.43 (0.37–0.50)
Occitanie	19.8 (16–25)	7.7 (5.3–11)	NS (0–95)	NS (0–31)	NS (0.82–1.1)
Provence-Alpes-Côte d'Azur	19.5 (16–25)	NS (0.6–2.2)	NS (0–320)	NS (0–67)	0.62 (0.54–0.71)
Other	37.6 (26–54)	NS (0.6–6.7)	NS (no values)	NS (no values)	NS (0.63–1.10)

*Model only analyzes tests performed after October 25, 2021; tests performed before that date are described in Appendix 1 Table 1 (https://wwwnc.cdc.gov/EID/article/28/7/22-0033-App1.pdf). NS, not significant.
†Age variable is centered and scaled (1 scaled unit corresponds to 56 years).

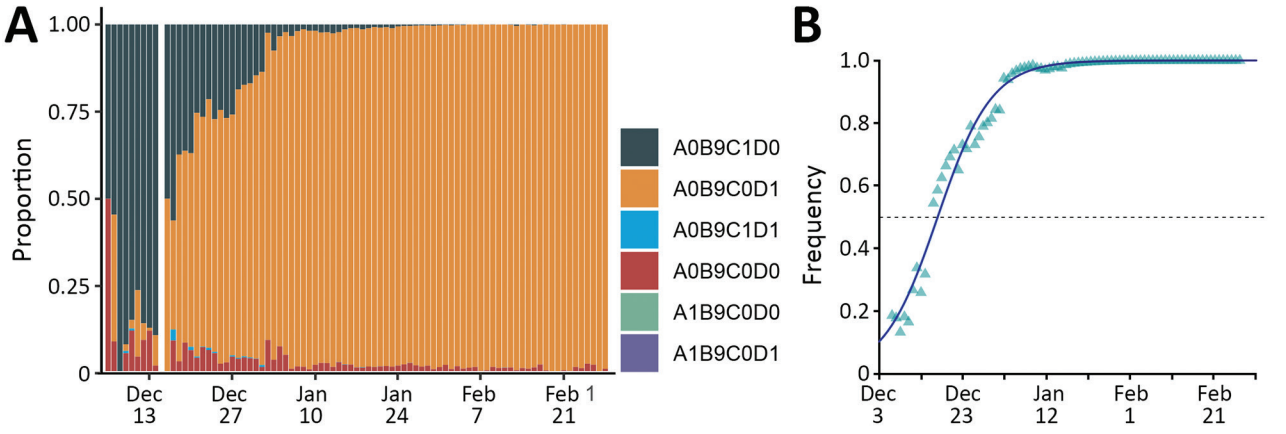

Figure 3. Monitoring and quantifying variant spread using ID Solutions Revolution tests (N = 193,256), France, December 6, 2021–February 28, 2022. A) Raw proportion of the test outcomes. B) Estimated frequency of A0B9C0D1 relative to the sum of A0B9C0D1 and A0B9C1D0 tests in France. Raw occurrence data from panel A is stratified by region in Appendix 1 Figure 2 (https://wwwnc.cdc.gov/EID/article/28/7/22-0033-App1.pdf). Test designations indicate the absence of a mutation by a 0 and its presence by 1 (9 means the mutation was not tested); mutations are the same as in Figure 2 and D is S:417N; A0B9C0D1 mostly corresponds to Omicron variant, A0B9C1D0 to Delta variant and A0B9C1D1 to Omicron-Delta coinfection.

frequencies. This shift in different regions can explain the second increase in growth advantage of A0B0C0 tests observed in November (Figure 2, panel C).

Sequencing Reveals a Shift from BA.1 to BA.2

Because variant screening tests only target 3 mutations, we analyzed whole-genome sequences of ≈5% of the positive samples (Figure 5, panel A). This analysis revealed that before October 2021, A0B0C0 tests mostly originated from Delta variant infections, whereas in November they originated from rare lineages or from the 20C lineage. A more precise analysis shows that these mostly correspond to the B.1.640 lineage. Beginning near the end of November, half of these tests were associated with the Omicron variant; this percentage increased to >80% during December.

Beginning in the second week of January 2022, some of the screening outcomes consistent with Omicron (A0B9C0D1) were associated with the BA.2 variant (Figure 5, panel B). This proportion increased over the next several weeks. Using the sequencing data, we estimated a growth advantage of BA.2 over the BA.1 Omicron lineage of 48.9% (95% CI 44.2%–53.6%). BA.2 accounted for most variants at the end of February, meaning that the Omicron variant BA.1 lineage only dominated the epidemic in France for <3 months (Figure 5, panel B).

Ct Differences

For the tests performed during December 16, 2021–February 28, 2022, we used a linear model to explore differences in Ct values between variants. All the covariates were significant according to ANOVA with a type II error (Appendix 1 Table 1). Ct values tended to decrease with age or to be lower in samples from hospitals (Appendix 1 Table 2), which is consistent with earlier results (*14*). Furthermore, A0B9C0D1 tests exhibited significantly higher Ct values than

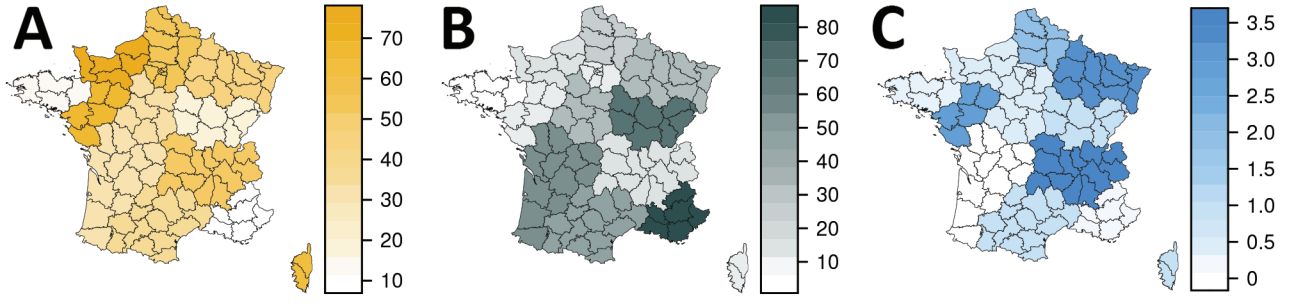

Figure 4. Frequency of A0B9C0D1 (A), A0B9C1D0 (B), and A0B9C1D1 (C) SARS-CoV-2 variant test results in mainland regions of France during week 51 of 2021. The colors show the prevalences (in percentages), which are corrected for covariates (age and sampling context). Includes 7,166 tests of the tests shown in Figure 3 but performed December 20–26, 2021. Test designation is the same as in Figure 3.

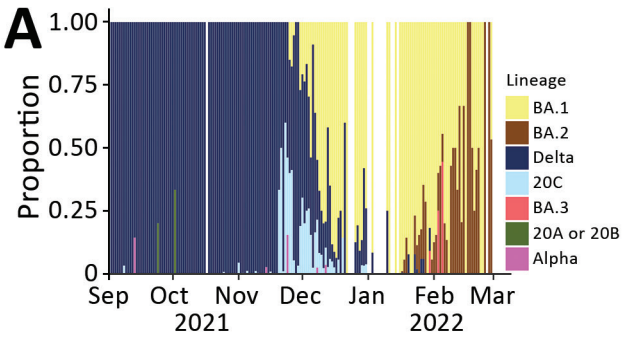

Figure 5. Monitoring and quantifying SARS-CoV-2 variant spread using whole-genome sequencing, France. A) Raw proportion of SARS-CoV-2 lineages inferred from whole-genome sequences of 16,973 samples. B) Estimated proportion and growth advantage of the BA.2 variant with respect to the BA.1 variant. Raw occurrence data from panel A is stratified by region in Appendix 1 Figure 3 (https://wwwnc.cdc.gov/EID/article/28/7/22-0033-App1.pdf).

A0B9C1D0; fitted median values were 22.1 versus 21.4 (Figure 6, panel A). This result suggests lower amounts of genetic material in the samples.

To further investigate these patterns, we analyzed the Ct values of the mutations targeted by the assay. We found that the Ct for the 417N mutation was higher in single infections (A0B9C0D1) than in co-infections (A0B9C1D1) (Figure 6, panel B). This finding is consistent with the greater ability of Omicron compared with Delta to infect immunized hosts, assuming that such breakthrough infections have a lower virus load (*27*,*28*).

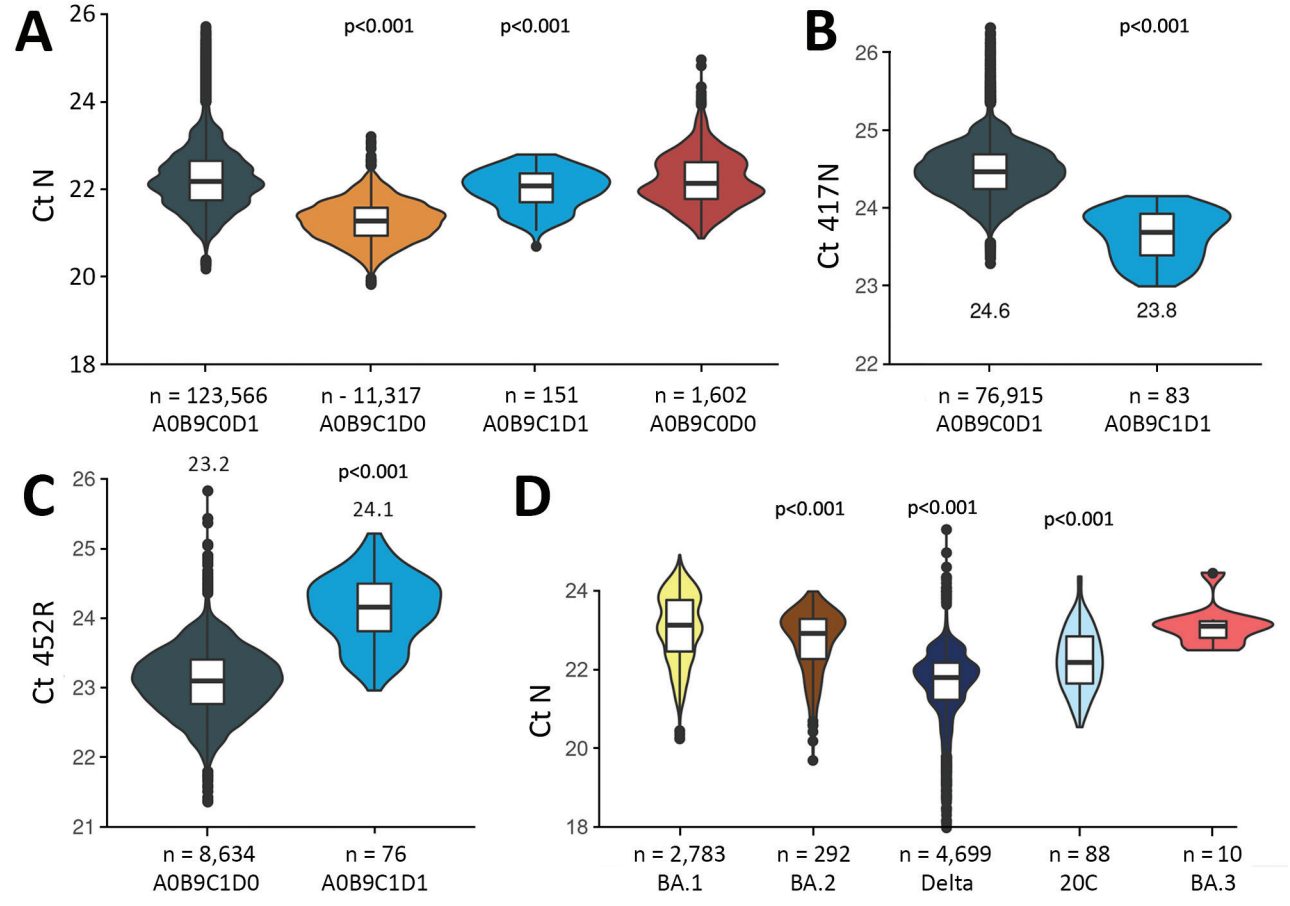

Figure 6. Ct values from the SARS-CoV-2 variant-specific screening quantitative PCR tests (N = 136,636), France, December 6, 2021–February 28, 2022. Ct values refer to the control (nucleoprotein) gene (A and D), 417N mutation (B), and 452R mutation (C). Values are shown as a function of the test outcome (A, B, and C) or the virus lineage (D). P values derived from a t-test where the reference variable is either A0B9C0D1 or BA.1. Boxes within violin plots show the median (horizontal line within box), 50% (box tops and bottoms), and 95% CIs (error bars). Tests were the same as in Figure 3, but only screening tests with Ct <28 were included to ensure robust screening results. Ct, cycle threshold; N, nucleoprotein gene.

For the 452R mutation, we found the opposite pattern (Figure 6, panel C).

Finally, we analyzed the Ct values of the control gene as a function of the virus lineage inferred from the NGS data (Figure 6, panel D). BA.1 samples had higher Ct values than did Delta samples. Furthermore, BA.2 samples had lower Ct values than did BA.1 samples.

Modeling Scenarios

On December 22, 2021, we incorporated the inferred growth advantage of Omicron/BA.1 over Delta into Covidsim (*21*) to explore an optimistic and a pessimistic scenario running through mid-March 2022. These scenarios differed in terms of the assumptions made regarding the reduction of Omicron virulence compared with Delta (3-fold vs. 2-fold) and vaccine protection against infection (75% vs. 40%) and severe illness (95% vs. 80%). Even though our assumption that the epidemic was under control at the end of 2021 was too optimistic, both the optimistic and the pessimistic scenarios showed that CCU activity was likely to remain high over January and February 2022, which proved to be accurate (Appendix 1, Appendix 1 Figure 4).

Given our estimations of the frequency of the Omicron/BA.2 sublineage in the population and its growth advantage over BA.1, we can predict the temporal increase of the epidemic Rt. We compared this predicted Rt with that calculated for the period March 1–10, 2022, using national hospital admission data, and found that from March 3 the ratio between the 2 was greater than unity (Figure 7, panel A). This result suggests that the epidemic growth cannot solely be explained by variant replacement and involves other drivers (e.g., the end of the holiday periods in some regions starting February 21, 2022).

Finally, on March 17, 2022, by using consolidated estimates of relative virulence (*6*) and vaccine effectiveness (*23*) for Omicron variants, we explored 2 prospective scenarios for nationwide COVID-19 CCU activity depending on the intensity of the relaxation of the control over the epidemic: Rt at the peak as 1.1 or 1.6 (Figure 7, panel B). We found that a new hospital peak was possible in the more pessimistic case, but its height remained below half of the peak experienced during the first Omicron wave in January.

Discussion

Variant-specific qPCR represents a flexible and cost-efficient surveillance method to obtain timely descriptions of SARS-CoV-2 epidemics. Thanks to a dense follow-up, we estimated that the Omicron variant spread in France with a 2-fold growth advantage over Delta (i.e., higher than that recorded for the Delta variant vs. the Alpha variant in June 2021) (*18*). This finding is consistent with estimates from South Africa (C.A.B. Pearson et al., unpub. data) and the United Kingdom (S. Abbott, et al., unpub. data, https://doi.org/10.1101/2022.01.08.22268920). Some estimates from Denmark suggest even higher advantages but using a different method (relying on reproduction numbers and not growth rates) and GISAID genomic data, which means a lower coverage and potentially strong reporting delays (*29*).

Thanks to the WGS of 5% of the samples, we were able to confirm the nature of the variants spreading and to detect a replacement of the BA.1 Omicron lineage by the BA.2 with a growth advantage of ≈50% (the precise value depends on the serial interval used [19]). This finding is consistent with the qualitative trends reported from South Africa (*30*) and the United

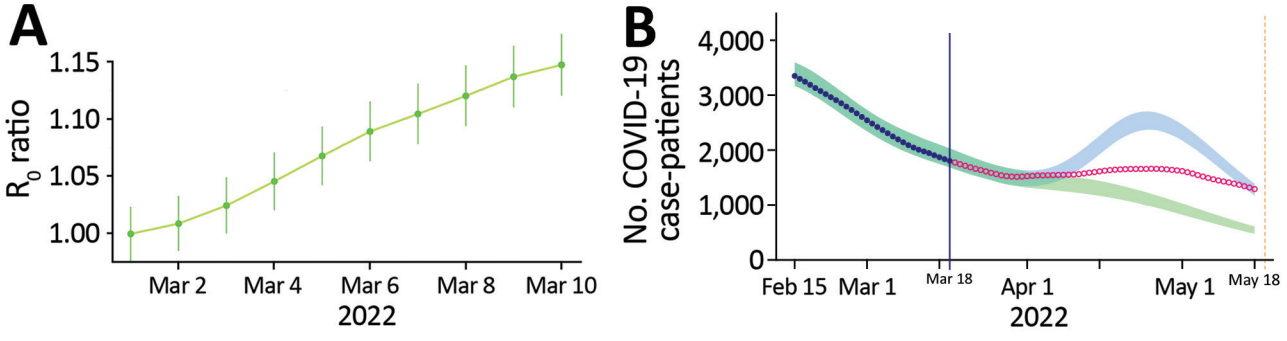

Figure 7. Analyzing and modeling the SARS-CoV-2 Omicron BA.2 epidemic wave in France. A) Ratio between the predicted and observed reproduction number (R0) based on BA.2 frequency and growth advantage. B) National critical care bed occupancy in 2 scenarios depending on baseline transmission increase. CIs are calculated from that of the frequency and growth advantage of BA.2 (Figure 5, panel B). The vertical blue line indicates the day the model was performed, the dark blue dots the data, and the shaded areas the 95% range of the model simulations. The 2 scenarios differ according to the capping of the increase of the baseline transmission rate, mimicking either a limited (green) or a strong (blue) easing preventive measures in March 2022 in France. Red open circles indicate data collected after the scenarios were modeled (i.e., not used in the inference or the modeling). The vertical yellow line indicated the last day the data were collected for the figure. Appendix 1 (https://wwwnc.cdc.gov/EID/article/28/7/22-0033-App1.pdf) further details model.

Kingdom (*10*) and from household data in Denmark (F.P. Lyngse et al., unpub. data). Note that these estimates tend to rely on the spike gene target failure, which is observed in a ThermoFisher assay for Omicron/BA.1 but not for Delta and not for BA.2. In our study, using variant-specific screening tests designed to target 3 specific mutations conferred a greater specificity of the results.

By analyzing qPCR Ct values, we found that samples from BA.1/Omicron infections had significantly higher Ct values than those from Delta infections. Although care must be taken when analyzing Ct values, especially for coronaviruses (*31*), this finding suggests a lower amount of virus genetic material in the samples. This result is intriguing given the large growth advantage of Omicron over Delta. A possible interpretation is that the Omicron variant is more prone to infecting immunized hosts (*2*,*3*) and, in vaccinated hosts, such breakthrough infections have been reported to have lower virus load than infections of nonvaccinated hosts (*27*,*28*).

We did not have access to the vaccination status of the persons from whom samples were taken. However, a potential overrepresentation of immunized hosts among Omicron infections is consistent with the lower values for the Ct associated with the 417N mutation in Delta–Omicron co-infections compared with Omicron monoinfections. Because Delta is less prone to immune evasion than Omicron, we expect the proportion of immunized hosts to be low in co-infections.

A limitation of our approach is that we cannot readily identify the origin of the growth advantage of BA.2 with respect to BA.1. This advantage could be caused by a shorter generation time for BA.2 infections (*10*), which is consistent with our finding that BA.2 samples have lower Ct values than those for BA.1 samples. Furthermore, although we do control for the sampling date as a covariate, this difference could reflect the epidemic trend given that Ct values are expected to be lower in expanding epidemics (*14*,*20*).

Our study highlights both the strengths and weaknesses of variant-specific screening assays (also sometimes called allele-specific reverse transcription qPCR). The advantage is that these assays enable rapid detection of variant replacement (we could detect a signal in the A0B0C0 tests in early December, at a time when the Omicron frequency <5%). However, the information about the circulating lineage is limited and, for example, the onset of the BA.2 wave in France could only be detected by using sequencing data. Furthermore, test interpretations vary with time. Before September 2020, some A0B0C0 tests were caused by the Alpha variant and by the Delta variant with a low Ct. In late October, before being associated with Omicron infections, most of these tests were probably attributable to lineage B.1.640, first detected in the Democratic Republic of the Congo (*32*). Temporal variations (Figure 2, panel B) may also originate from spatial heterogeneity; growth advantages are calculated for large administrative units, and variant epidemics can be at different stages in different regions. Finally, delays in data reporting can matter in the initial stages of variant epidemics.

Beyond nowcasting (near–real-time estimating) variant replacement rates, epidemiologic models represent a powerful tool to explore prospective scenarios. By combining our estimates of growth advantage with literature data, especially on vaccine protection, we showed that the decrease in Omicron virulence (*6*) was not sufficient to allow for a steep decrease in critical COVID-19 activity in hospitals in France >1 month before the reported incidence peak, hence helping CCU to anticipate the number of beds necessary and plan for the return to regular activity for the other hospital sectors.

Acknowledgments

The authors thank the Experimental and Theoretical Evolution team from Maladies Infectieuses et Vecteurs: Écologie, Génétique, Évolution et Contrôle, University of Montpellier, for discussion, as well as the EMERGEN consortium (complete member list in Appendix 2, https://wwwnc.cdc.gov/EID/article/28/7/22-0033-App2.xlsx).

This project was supported by the Occitanie Region and the Agence Nationale de la Recherche through a grant to the PhyEpi Project and by Agence Nationale de la Recherche Maladies Infectieuses Émergentes to the MODVAR project (grant no. ANRS0151).

About the Author

Dr. Sofonea is associate professor at University of Montpellier and heads the Experimental and Theoretical Evolution team. His research interests include epidemiology, stochastic modelling, spatial data analysis, and public health.

References

1. Viana R, Moyo S, Amoako DG, Tegally H, Scheepers C, Althaus CL, et al. Rapid epidemic expansion of the SARS-CoV-2 Omicron variant in southern Africa. Nature. 2022;603:679–86. https://doi.org/10.1038/s41586-022-04411-y
2. Planas D, Saunders N, Maes P, Guivel-Benhassine F, Planchais C, Buchrieser J, et al. Considerable escape of

SARS-CoV-2 Omicron to antibody neutralization. Nature. 2022;602:671–5. https://doi.org/10.1038/s41586-021-04389-z
3. Takashita E, Kinoshita N, Yamayoshi S, Sakai-Tagawa Y, Fujisaki S, Ito M, et al. Efficacy of antibodies and antiviral drugs against Covid-19 Omicron variant. N Engl J Med. 2022;386:995–8. https://doi.org/10.1056/NEJMc2119407
4. WHO Collaborating Centre for Infectious Disease Modelling, MRC Centre for Global Infectious Disease Analysis, Jameel Institute, Imperial College London. Report 50: hospitalisation risk for Omicron cases in England. 2021 Dec 21 [cited 2022 May 6]. http://www.imperial.ac.uk/medicine/departments/school-public-health/infectious-disease-epidemiology/mrc-global-infectious-disease-analysis/covid-19/report-50-severity-omicron
5. Maslo C, Friedland R, Toubkin M, Laubscher A, Akaloo T, Kama B. Characteristics and outcomes of hospitalized patients in South Africa during the COVID-19 Omicron wave compared with previous waves. JAMA. 2022;327:583–4. https://doi.org/10.1001/jama.2021.24868
6. Nyberg T, Ferguson NM, Nash SG, Webster HH, Flaxman S, Andrews N, et al.; COVID-19 Genomics UK (COG-UK) consortium. Comparative analysis of the risks of hospitalisation and death associated with SARS-CoV-2 omicron (B.1.1.529) and delta (B.1.617.2) variants in England: a cohort study. Lancet. 2022;399:1303–12. https://doi.org/10.1016/S0140-6736(22)00462-7
7. Meng B, Abdullahi A, Ferreira IATM, Goonawardane N, Saito A, Kimura I, et al.; CITIID-NIHR BioResource COVID-19 Collaboration; Genotype to Phenotype Japan (G2P-Japan) Consortium; Ecuador-COVID19 Consortium. Altered TMPRSS2 usage by SARS-CoV-2 Omicron impacts infectivity and fusogenicity. Nature. 2022;603:706–14. https://doi.org/10.1038/s41586-022-04474-x
8. Hui KPY, Ho JCW, Cheung MC, Ng KC, Ching RHH, Lai KL, et al. SARS-CoV-2 Omicron variant replication in human bronchus and lung ex vivo. Nature. 2022;603:715–20. https://doi.org/10.1038/s41586-022-04479-6
9. Suzuki R, Yamasoba D, Kimura I, Wang L, Kishimoto M, Ito J, et al.; Genotype to Phenotype Japan (G2P-Japan) Consortium. Attenuated fusogenicity and pathogenicity of SARS-CoV-2 Omicron variant. Nature. 2022;603:700–5. https://doi.org/10.1038/s41586-022-04462-1
10. UK Health Security Agency. SARS-CoV-2 variants of concern and variants under investigation in Technical briefing 36. 2022 Feb 11 [cited 2022 May 6]. https://assets.publishing.service.gov.uk/government/uploads/system/uploads/attachment_data/file/1056487/Technical-Briefing-36-22.02.22.pdf
11. Espenhain L, Funk T, Overvad M, Edslev SM, Fonager J, Ingham AC, et al. Epidemiological characterisation of the first 785 SARS-CoV-2 Omicron variant cases in Denmark, December 2021. Euro Surveill. 2021;26:2101146. https://doi.org/10.2807/1560-7917.ES.2021.26.50.2101146
12. Ritchie H, Rodés-Guirao L, Appel C, Giattino C, Ortiz-Ospina E, Hasell J, et al. Coronavirus pandemic (COVID-19). Our World in Data. 2020 [cited 2022 May 6]. https://ourworldindata.org/coronavirus
13. Haim-Boukobza S, Roquebert B, Trombert-Paolantoni S, Lecorche E, Verdurme L, Foulongne V, et al. Detecting rapid spread of SARS-CoV-2 variants, France, January 26–February 16, 2021. Emerg Infect Dis. 2021;27:1496–9. https://doi.org/10.3201/eid2705.210397
14. Alizon S, Selinger C, Sofonea MT, Haim-Boukobza S, Giannoli JM, Ninove L, et al.; SFM COVID-19 study group. Epidemiological and clinical insights from SARS-CoV-2 RT-PCR crossing threshold values, France, January to November 2020. Euro Surveill. 2022;27:2100406. https://doi.org/10.2807/1560-7917.ES.2022.27.6.2100406
15. Chevin LM. On measuring selection in experimental evolution. Biol Lett. 2011;7:210–3. https://doi.org/10.1098/rsbl.2010.0580
16. Davies NG, Abbott S, Barnard RC, Jarvis CI, Kucharski AJ, Munday JD, et al.; CMMID COVID-19 Working Group; COVID-19 Genomics UK (COG-UK) Consortium. Estimated transmissibility and impact of SARS-CoV-2 lineage B.1.1.7 in England. Science. 2021;372:eabg3055. https://doi.org/10.1126/science.abg3055
17. Volz E, Mishra S, Chand M, Barrett JC, Johnson R, Geidelberg L, et al.; COVID-19 Genomics UK (COG-UK) consortium. Assessing transmissibility of SARS-CoV-2 lineage B.1.1.7 in England. Nature. 2021;593:266–9. https://doi.org/10.1038/s41586-021-03470-x
18. Alizon S, Haim-Boukobza S, Foulongne V, Verdurme L, Trombert-Paolantoni S, Lecorche E, et al. Rapid spread of the SARS-CoV-2 Delta variant in some French regions, June 2021. Euro Surveill. 2021;26:2100573. https://doi.org/10.2807/1560-7917.ES.2021.26.28.2100573
19. Nishiura H, Linton NM, Akhmetzhanov AR. Serial interval of novel coronavirus (COVID-19) infections. Int J Infect Dis. 2020;93:284–6. https://doi.org/10.1016/j.ijid.2020.02.060
20. Hay JA, Kennedy-Shaffer L, Kanjilal S, Lennon NJ, Gabriel SB, Lipsitch M, et al. Estimating epidemiologic dynamics from cross-sectional viral load distributions. Science. 2021;373:eabh0635. https://doi.org/10.1126/science.abh0635
21. Sofonea MT, Reyné B, Elie B, Djidjou-Demasse R, Selinger C, Michalakis Y, et al. Memory is key in capturing COVID-19 epidemiological dynamics. Epidemics. 2021;35:100459. https://doi.org/10.1016/j.epidem.2021.100459
22. Sofonea MT, Alizon S. Anticipating COVID-19 intensive care unit capacity strain: a look back at epidemiological projections in France. Anaesth Crit Care Pain Med. 2021;40:100943. https://doi.org/10.1016/j.accpm.2021.100943
23. UK Health Security Agency. COVID-19 vaccine surveillance report, week 10. 2022 Mar 10 [cited 2022 May 6]. https://assets.publishing.service.gov.uk/government/uploads/system/uploads/attachment_data/file/1060787/Vaccine_surveillance_report_-_week_10.pdf
24. Hall VJ, Foulkes S, Charlett A, Atti A, Monk EJM, Simmons R, et al.; SIREN Study Group. SARS-CoV-2 infection rates of antibody-positive compared with antibody-negative health-care workers in England: a large, multicentre, prospective cohort study (SIREN). Lancet. 2021;397:1459–69. https://doi.org/10.1016/S0140-6736(21)00675-9
25. Cori A, Ferguson NM, Fraser C, Cauchemez S. A new framework and software to estimate time-varying reproduction numbers during epidemics. Am J Epidemiol. 2013;178:1505–12. https://doi.org/10.1093/aje/kwt133
26. Salje H, Tran Kiem C, Lefrancq N, Courtejoie N, Bosetti P, Paireau J, et al. Estimating the burden of SARS-CoV-2 in France. Science. 2020;369:208–11. https://doi.org/10.1126/science.abc3517
27. Blanquart F, Abad C, Ambroise J, Bernard M, Cosentino G, Giannoli JM, et al. Characterisation of vaccine breakthrough infections of SARS-CoV-2 Delta and Alpha variants and within-host viral load dynamics in the community, France, June to July 2021. Euro Surveill. 2021;26:2100824. https://doi.org/10.2807/1560-7917.ES.2021.26.37.2100824
28. Puhach O, Adea K, Hulo N, Sattonnet P, Genecand C, Iten A, et al. Infectious viral load in unvaccinated and vaccinated individuals infected with ancestral, Delta

or Omicron SARS-CoV-2. Nat Med. 2022 Apr 8 [Epub ahead of print]. https://doi.org/10.1038/s41591-022-01816-0
29. Ito K, Piantham C, Nishiura H. Relative instantaneous reproduction number of Omicron SARS-CoV-2 variant with respect to the Delta variant in Denmark. J Med Virol. 2022;94:2265–8. https://doi.org/10.1002/jmv.27560
30. Wolter N, Jassat W, Walaza S, Welch R, Moultrie H, Groome M, et al. Early assessment of the clinical severity of the SARS-CoV-2 omicron variant in South Africa: a data linkage study. Lancet. 2022;399:437–46. https://doi.org/10.1016/S0140-6736(22)00017-4
31. Michalakis Y, Sofonea MT, Alizon S, Bravo IG. SARS-CoV-2 viral RNA levels are not 'viral load'. Trends Microbiol. 2021;29:970–2. https://doi.org/10.1016/j.tim.2021.08.008
32. Mastrovito B, Naimi C, Kouam L, Naudot X, Fournier L, Spaccaferri G, et al. Investigation of outbreak cases infected with the SARS-CoV-2 B.1.640 variant in a fully vaccinated elderly population, Normandy, France, November to December 2021. Euro Surveill. 2022;27:2200078. https://doi.org/10.2807/1560-7917.ES.2022.27.6.2200078

Address for correspondence: Samuel Alizon, Center for Interdisciplinary Research in Biology, Collège de France, 11 place Marcelin Berthelot, 75005 Paris, France; email: samuel.alizon@cnrs.fr

Article DOI: https://doi.org/10.3201/eid2807.220033

Analyzing and Modeling the Spread of SARS-CoV-2 Omicron Lineages BA.1 and BA.2, France, September 2021–February 2022

Appendix 1

Multinomial Log-Linear Model

To perform the multinomial log-linear model, we used the multinom function from the nnet R package. This function uses neural networks to perform model selection in a stepwise manner starting from the null model (i.e., without any predictor).

The model formula was the following: variant ~ age + assay + location_sampling + date:region, where age is the age of the individual (which is treated as an integer and centered and scaled), location_sampling is a binary variable indicating whether the sample was collected in a hospital or not, assay corresponds to the type of screening test used, date is the sampling date (which is treated as an integer and centered and scaled), and region is the French administrative region of residency.

The multinom function uses an AIC criterion to identify the best model and returns the estimated multinomial logistic regression coefficients as well as their standard error (SE).

These can be used to calculate a z-test statistic, which is simply the ratio of the coefficient value to the SE. From there, we can construct a p-value, $p > |z|$, which is the probability the z-test statistic would be observed under the null hypothesis and assuming that z follows a normal distribution. Here, we use a classical significance threshold of $\alpha = 5\%$. When the p-value is smaller than α, the null hypothesis can be rejected and the parameter is considered to be significant.

Note that an alternative approach could be to calculate the 95% confidence interval for the coefficient value of the multinomial model using the SE and a critical value on the standard normal distribution.

To give a more intuitive interpretation of the results, we compute the relative risk ratios (RRR) by taking the exponential of the coefficient values of the model. The RRR reflects, for a given variable, how the risk of belonging to one of the outcomes (here variant detection) varies compared to the control group.

Further details about multinomial log-linear models and their interpretations can be found at https://stats.idre.ucla.edu/stata/output/multinomial-logistic-regression/.

Selection Advantage Estimation

The selection advantage is estimated from the Malthusian growth rate of the 'population' of variant-specific tests. More precisely, following methods developed in population genetics to estimate the selection coefficient of a mutant allele compared to a wild type allele (*1*), and following earlier studies in epidemiology (*2–4*), we calculate the selection coefficient s by fitting a logistic growth model to the time series of variant frequency.

Indeed, provided that the selection coefficient s does not var.y over time, and by denoting p(t) the frequency of an allele (here screening test result A0B0C0 or A0B0C1) in the population (here all tests with results A0B0C0 or A0B0C1), we have the following relationship:

$$s = \frac{d}{dt} log\left(\frac{p(t)}{1-p(t)}\right) \text{ (S1)}$$

Note that this value needs to be scaled with respect to the generation time T, which is here obtained from the serial interval calculated by Nishiura et al. (*5*). Overall, the transmission advantage sT of A0B0C0 tests over A0B0C1 tests is given by the formula sT = s T.

To estimate s, for each region of interest separately, we first perform a generalized linear model (GLM) with a binomial distribution of the residuals (i.e., a logistic regression) where the response variable is the test result (A0B0C0 or A0B0C1) and the covariates are the age of the individual (which is treated as an integer and centered and scaled), the assay used for the test, the sampling date (which is treated as an integer and centered and scaled), and the sampling region,

which is the French administrative region. We then use the fitted values from the GLM to perform the fit of the logistic growth function.

We use 21 days windows to estimate transmission advantage, which corresponds to two 95% confidence intervals (CI) of the serial interval used. This duration was chosen to be long enough to avoid false-positive signals and short-enough to allow for rapid detection of variations in s.

We also inferred the transmission advantage using the updated version of the R package EpiEstim (*6*) available at https://github.com/mrc-ide/EpiEstim. We only consider A0B0C0 and A1B1C1 test results and assume that both have the same serial interval (that from [*5*]).

Further details about the implementation of the inference can be found in the Supplementary R script with the Supplementary data.

Cycle Threshold Analyses

Statistically, we use a linear model with the following formula:
Ct ~ age + variant + location_sampling + date*region, where age is the age of the individual (which is treated as an integer and centered and scaled), variant is the outcome of the screening test, location_sampling is a binary variable indicating whether the sample was collected in a hospital or not, date is the sampling date (which is treated as an integer and centered and scaled), and region is the French administrative region of residency. We also include interactions between the region and the sampling date in the model to capture variations in Ct values that could be linked to differences in epidemic reproduction numbers. Indeed, growing epidemics can be associated with lower Ct values than declining epidemics (*7*,*8*).

We used a likelihood ratio test to compare this model and a model without the variant covariate. Adding this covariate does significantly improved the model.

Covariate significance was assessed using an analysis of variance (ANOVA) with a type II error using the Anova function from the car package in R.

The estimated marginal means (EMMs) for the Ct values associated with the screening tests results were computed using the emmeans function from the eponym R package.

Mathematical Modeling

The structure of the mathematical framework used is shown in Figure 6, panel A in the main text. Each age class is split into compartments (depicted by the figurines in the chart) according to their infectious, clinical and immunological statuses. Susceptible individuals (in yellow) can be infected if exposed to the SARS-CoV-2 by infected individuals (in pink) in the community (note that aged care facilities are not included). A fraction of the infected individuals develop a critical COVID-19 form, defined as requiring critical care and/or leading to hospital death (for simplicity, only patients admitted in critical care are depicted on the flowchart). Vaccination is implemented following the VAC-SI time series (data from Santé Publique France) and assumed to reduce the probability of three events, namely being infected if exposed, transmitting the virus if infected and developing critical complications if infected. Additionally, we assume that all individuals having recovered from a post-vaccine infection are immunized, contrary to unvaccinated individuals a fraction of which can become infected again (*9*). Formal and parameterization details are provided in (*10*), the system of which was updated according to the flowchart in Figure 6, panel A.

The COVIDSIM Framework

The main structure of COVIDSIM has been described in details in an earlier study (*10*).

In short, the underlying model is structured in discrete time and uses COVID-19 critical care unit (CCU) incidence and prevalence data, as well as mortality data, to estimate key parameters of the epidemic in France. Individuals can move between compartments that var.y in terms of infectivity (Figure 6, panel A in the main text). The transition between compartments depends on the time spent in each compartment meaning that the model is non-Markovian (i.e., it captures ‘memory’ effects).

For simplicity, the transmission model is not stratified by age. However, the probability of developing critical forms, being admitted to critical care, and dying from COVID-19 is age-stratified according to published data (*11*). In general, the model parameters correspond to the French epidemic: their initial values are derived from literature data, technical reports or preliminary work, and are then regularly adjusted to reflect hospital dynamics (*12*).

Vaccination follows the French national campaign data (VAC-SI data from Santé publique France, available at https://www.data.gouv.fr) with simplifying assumptions. In particular, we assume that all vaccines act as a 1-dose vaccine, using the date of the second dose as the date of vaccination. The proportion of people already infected is the result of the model's reconstruction of the epidemic.

The level of protection of the hosts depends on the type of protection. Natural post-infection is assumed to confer full protection to 85% of the individual, the 15% others remaining immunologically naïve. For vaccine immunity, we distinguish between different types of protection. In the most optimistic scenarios, we assume protection of 80% against infection and of 95% against the occurrence of severe forms if infected. Furthermore, based on our earlier investigations of the French epidemic (M.T. Sofonea et al., unpub. data, https://osf.io/6ebxu), we assume that the drop in infectiousness in so-called breakthrough infections in vaccinated individuals is 50%.

Regarding the Omicron wave more specifically, our biologic knowledge improved over the duration of this study. The first modeling work was performed on December 22, 2021, at a time when the vaccine evasion and severity properties of Omicron were poorly known. The second modeling work was performed on 17 March 2022 and we were able to lean on more detailed data regarding the differences between Delta and Omicron in terms of severity (*13*) and vaccine protection (*14*). The assumptions made in these two works a further described below.

Importantly, given the timescales considered, we neglect immune waning in the model, which means that on a long time scale our estimates could be over-optimistic. We also do not include seasonal variations, which have been shown to explain approx. 20% of the variance in reproduction number Rt (*15*).

Late 2021 Scenarios: The BA.1 Wave

The goal of this first model, which was performed on December 22, 2021, was to explore the impact of the Omicron variant on national CCU activity. This model was not intended to predict the future but rather to generate trends under assumptions that are arbitrarily optimistic for the most part. In particular, we made the following assumptions:

- The set of people vaccinated is homogeneous (e.g., no stratification according to the number of doses), which can be interpreted as assuming that the 3rd dose is rapidly generalized to the whole population.
- There is no decrease in immune protection, i.e., waning, over time.
- The proportion of previously infected people that Omicron can reinfect is identical to that of Delta (i.e., 15% [*9*]).
- The generation time (number of days between the moment a person is infected and the moment he/she infects another person) is the same for all the variants.
- The duration of stay in critical care remains unchanged.
- There are no 'New Year's Eve', 'holiday', 'back-to-school' or meteorological effects on the epidemic spread.
- The epidemic reproduction number (Rt) grows from 1.08 on December 23, 2021, to 1.25 on December 28, and to 1.5 on January 7, 2022, which corresponds to a 10% decrease in the reproduction number at the peak compared to what would be expected by extrapolating the estimated Omicron growth from the screening data at the time.
- From 15 January onward, a slowdown in the epidemic occurs due to public health interventions, spontaneous behavioral changes, and/or natural saturation related to spatial structure with a drop in Rt to 0.95.

In this model, we also incorporated the growth advantage of Omicron/BA.1 versus Delta and the estimated frequency of Omicron/BA.1 in the population estimated from the variant-specific screening test data (Figure 2, panel C in the main text). Since COVIDSIM is a single-strain model, the replacement of Delta by Omicron was modeled by adjusting the transmission rate, immune protection, and severity parameters as a function of the increase in the proportion of Omicron infections.

We then simulated two scenarios that differed in their assumptions regarding the differences between Omicron and Delta in terms of vaccine protection and virulence:

1. An “optimistic” scenario, with a 3-fold reduction in the probability of developing a critical form compared to Delta, a 75% vaccine protection against infection, and 95% protection against critical forms (therefore, an excellent effect of the 3rd dose).

2. A “pessimistic” scenario, where the probability of developing a critical form was only divided by 2 compared to Delta, and where the vaccine protection was only 40% against infection and 80% against critical forms.

Most of the assumptions made here, e.g., that on January 15, 2022, the Omicron epidemic would be decreasing, were rather optimistic. Therefore, the goal of these scenarios was to provide a lower bound. In other words, we wanted to estimate the minimal consequences on CCU of the Omicron variant wave.

The results of the model are shown in Appendix Figure 4.

2022 Scenarios: The BA.2 Wave

Detailed data about the Omicron/BA.1 was rapidly available and allowed us to carefully parameterize our COVIDSIM model. In particular, based on this new severity and vaccine protection data, we could assume a 3.2 reduction in infection severity for BA.1 or BA.2 with respect to Delta (*13*), and a 75% protection against infection, and a 95% protection against severe infection forms for vaccinated individuals with 2 doses and a booster (*14*).

Furthermore, epidemiologic data revealed that the serial interval, i.e., the distribution of the number of days between two infections (a proxy for the generation time) was lower for Omicron/BA.2 than for BA.1 (Figure 13 in [*16*]). This updated information was included in our second model.

As in the first model, we incorporated the frequency time series and growth advantage of BA.2 versus BA.1 estimated from the sequencing data (Figure 4, panel B in the main text) into the model.

Our analysis of the BA.2 wave included two steps:

First, from the French hospital admission data (available at https://www.data.gouv.fr/fr/datasets/donnees-hospitalieres-relatives-a-lepidemie-de-covid-19), we estimated the temporal reproduction number (Rt) of the epidemic using the EpiEstim package

in R (*6*). The estimated value for March 1, 2021, was R2022–03–01 = 0.83. We then compared this reference number to the Rt values predicted from our model based on the frequency and growth advantage of the Omicron variant. The results are shown in Figure 6, panel B.

Second, we explored two alternative scenarios over a medium time scale by varying the intensity of the control over the epidemic:

1. In an optimistic scenario, the control was assumed to remain strong and the Rt peaked at a value of 1.1.
2. In the pessimistic scenario, control measured were assumed to be strongly alleviated leading to an increase of Rt to 1.6.

As in the first models, these scenarios are not intended to predict the future but to explore an upper boundary regarding the potential consequences of an Omicron/BA.2 wave in France.

References

1. Chevin LM. On measuring selection in experimental evolution. Biol Lett. 2011;7:210–3. PubMed https://doi.org/10.1098/rsbl.2010.0580

2. Davies NG, Abbott S, Barnard RC, Jarvis CI, Kucharski AJ, Munday JD, et al.; CMMID COVID-19 Working Group; COVID-19 Genomics UK (COG-UK) Consortium. Estimated transmissibility and impact of SARS-CoV-2 lineage B.1.1.7 in England. Science. 2021;372:eabg3055. PubMed https://doi.org/10.1126/science.abg3055

3. Volz E, Mishra S, Chand M, Barrett JC, Johnson R, Geidelberg L, et al.; COVID-19 Genomics UK (COG-UK) consortium. Assessing transmissibility of SARS-CoV-2 lineage B.1.1.7 in England. Nature. 2021;593:266–9. PubMed https://doi.org/10.1038/s41586-021-03470-x

4. Alizon S, Haim-Boukobza S, Foulongne V, Verdurme L, Trombert-Paolantoni S, Lecorche E, et al. Rapid spread of the SARS-CoV-2 Delta variant in some French regions, June 2021. Euro Surveill. 2021;26:2100573. PubMed https://doi.org/10.2807/1560-7917.ES.2021.26.28.2100573

5. Nishiura H, Linton NM, Akhmetzhanov AR. Serial interval of novel coronavirus (COVID-19) infections. Int J Infect Dis. 2020;93:284–6. PubMed https://doi.org/10.1016/j.ijid.2020.02.060

6. Cori A, Ferguson NM, Fraser C, Cauchemez S. A new framework and software to estimate time-varying reproduction numbers during epidemics. Am J Epidemiol. 2013;178:1505–12. PubMed https://doi.org/10.1093/aje/kwt133

7. Hay JA, Kennedy-Shaffer L, Kanjilal S, Lennon NJ, Gabriel SB, Lipsitch M, et al. Estimating epidemiologic dynamics from cross-sectional viral load distributions. Science. 2021;373:eabh0635. PubMed https://doi.org/10.1126/science.abh0635

8. Alizon S, Selinger C, Sofonea MT, Haim-Boukobza S, Giannoli JM, Ninove L, et al.; SFM COVID-19 study group. Epidemiological and clinical insights from SARS-CoV-2 RT-PCR crossing threshold values, France, January to November 2020. Euro Surveill. 2022;27:2100406. PubMed https://doi.org/10.2807/1560-7917.ES.2022.27.6.2100406

9. Hall VJ, Foulkes S, Charlett A, Atti A, Monk EJM, Simmons R, et al.; SIREN Study Group. SARS-CoV-2 infection rates of antibody-positive compared with antibody-negative health-care workers in England: a large, multicentre, prospective cohort study (SIREN). Lancet. 2021;397:1459–69. PubMed https://doi.org/10.1016/S0140-6736(21)00675-9

10. Sofonea MT, Reyné B, Elie B, Djidjou-Demasse R, Selinger C, Michalakis Y, et al. Memory is key in capturing COVID-19 epidemiological dynamics. Epidemics. 2021;35:100459. PubMed https://doi.org/10.1016/j.epidem.2021.100459

11. O'Driscoll M, Ribeiro Dos Santos G, Wang L, Cummings DAT, Azman AS, Paireau J, et al. Age-specific mortality and immunity patterns of SARS-CoV-2. Nature. 2021;590:140–5. PubMed https://doi.org/10.1038/s41586-020-2918-0

12. Salje H, Tran Kiem C, Lefrancq N, Courtejoie N, Bosetti P, Paireau J, et al. Estimating the burden of SARS-CoV-2 in France. Science. 2020;369:208–11. PubMed https://doi.org/10.1126/science.abc3517

13. Nyberg T, Ferguson NM, Nash SG, Webster HH, Flaxman S, Andrews N, et al.; COVID-19 Genomics UK (COG-UK) consortium. Comparative analysis of the risks of hospitalisation and death associated with SARS-CoV-2 omicron (B.1.1.529) and delta (B.1.617.2) variants in England: a cohort study. Lancet. 2022;399:1303–12. PubMed https://doi.org/10.1016/S0140-6736(22)00462-7

14. UK Health Security Agency. COVID-19 vaccine surveillance report, week 10. 2022 Mar 10 [cited 2022 May 6]. https://assets.publishing.service.gov.uk/government/uploads/system/uploads/attachment_data/file/1060787/Vaccine_surveillance_report_-_week_10.pdf

15. Smith TP, Flaxman S, Gallinat AS, Kinosian SP, Stemkovski M, Unwin HJT, et al. Temperature and population density influence SARS-CoV-2 transmission in the absence of nonpharmaceutical interventions. Proc Natl Acad Sci U S A. 2021;118:e2019284118. PubMed https://doi.org/10.1073/pnas.2019284118

16. UK Health Security Agency. SARS-CoV-2 variants of concern and variants under investigation in Technical briefing 36. 2022 Feb 11 [cited 2022 May 6]. https://assets.publishing.service.gov.uk/government/uploads/system/uploads/attachment_data/file/1056487/Technical-Briefing-36-22.02.22.pdf

Appendix 1 Table 1. Type II Anova model output for the linear model analyzing variations in Ct values*

Variable	Sum Sq	Df	F value
age	14429	1	1290.9
location_sampling	114	1	10.2
date	3670	1	328.3
region2	40363	12	300.9
variant	5084	3	151.6
date:region	6877	12	51.3
Residuals	1526899	136605	

*<0.001 indicates significance values lower than 0.001.

Appendix 1 Table 2. Output of the linear model analyzing variations in Ct values*

Dependent variable	Ct
age	−0.329***
	(0.009)
location_sampling:hospital	−0.175***
	(0.055)
date_scale	0.284***
	(0.022)
variant:A0B9C0D0	0.304***
	(0.087)
variant:A0B9C1D0	−0.746***
	(0.036)
variant:A0B9C1D1	−0.084
	(0.273)
region:Auvergne-Rhône-Alpes	−0.375**
	(0.160)
region:Bourgogne-Franche-Comté	−1.066***
	(0.060)
region:Bretagne	0.424***
	(0.059)
region:Centre-Val de Loire	0.620***
	(0.052)
region:Corse	−0.852***
	(0.050)
region:Grand Est	−1.289***
	(0.051)
region:Hauts-de-France	−0.943***
	(0.034)
region:Normandie	0.161***
	(0.035)
region:Nouvelle-Aquitaine	−1.026***
	(0.042)
region:Occitanie	−0.648***
	(0.047)
region:Pays de la Loire	−0.436***
	(0.111)

Dependent variable	Ct
region:Provence-Alpes-Côte d'Azur	−0.452***
	(0.033)
date*region:Auvergne-Rhône-Alpes	−0.303*
	(0.158)
date*region:Bourgogne-Franche-Comté	−0.338***
	(0.060)
date*region:Bretagne	0.647***
	(0.051)
date*region:Centre-Val de Loire	0.258***
	(0.051)
date*region:Corse	0.126***
	(0.047)
date*region:Grand Est	−0.466***
	(0.056)
date*region:Hauts-de-France	−0.321***
	(0.033)
date*region:Normandie	−0.048
	(0.036)
date*region:Nouvelle-Aquitaine	−0.329***
	(0.043)
date*region:Occitanie	−0.243***
	(0.046)
date*region:Pays de la Loire	−0.626***
	(0.107)
date*region:Provence-Alpes-Côte d'Azur	−0.102***
	(0.033)
Constant	22.669***
	(0.025)
Observations	136,636
R2	0.046
Adjusted R2	0.045
Residual Std. Error	3.343 (df = 136605)
F Statistic	217.335*** (df = 30; 136605)

*For each covariate, we show the estimated value of the effect and its standard deviation in parentheses. Significance level are shown using the following code: *p < 0.1, **p < 0.05 and ***p < 0.01. The table was formatted with the stargazer R package.

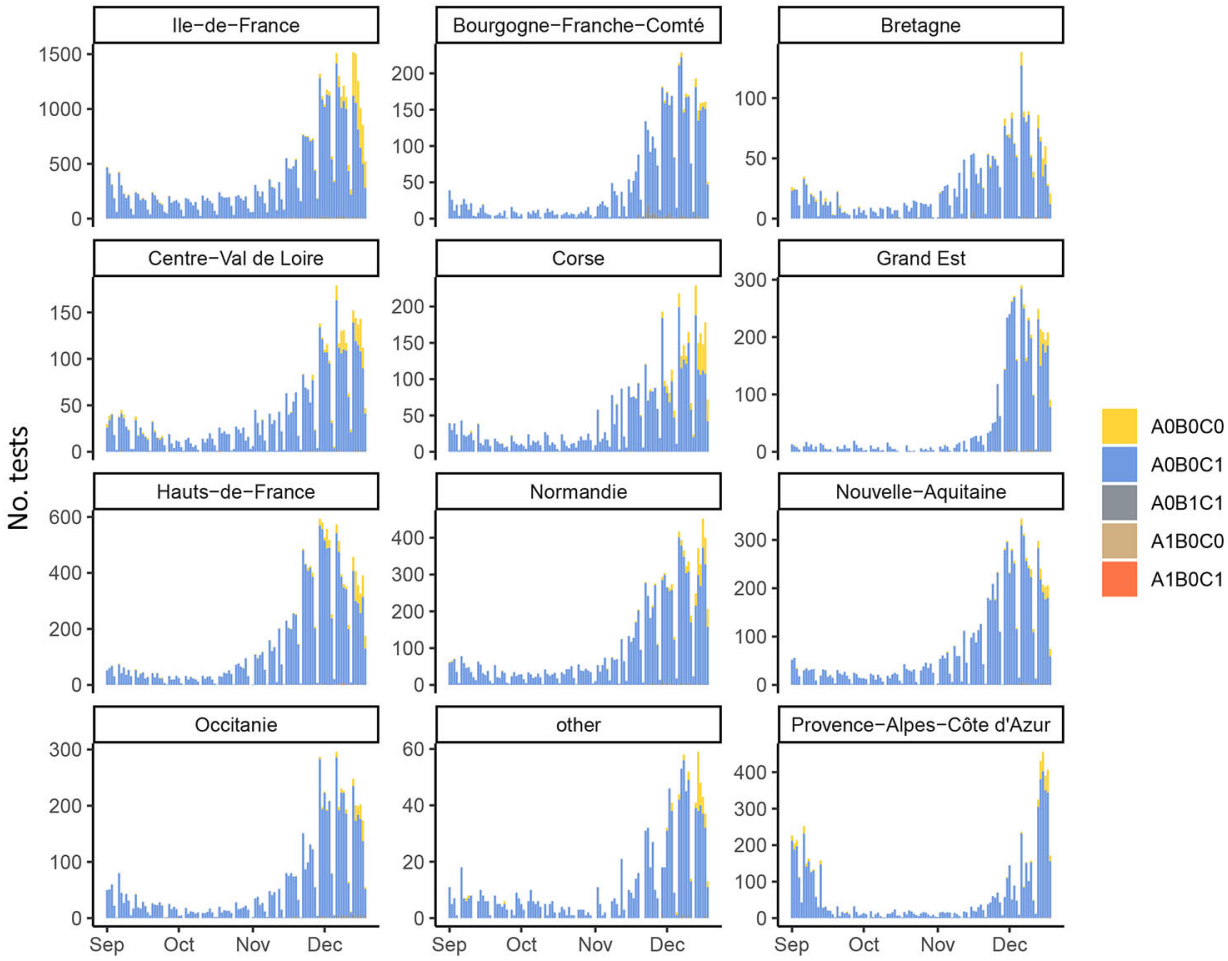

Appendix 1 Figure 1. Variant-specific screening test incidence data per French region. The color indicates the test result. Regions with too few tests are pooled in the “other” category. Notice that the epidemic was declining until mid-October 2021. Furthermore, the proportion of A0B0C0 tests varies across regions.

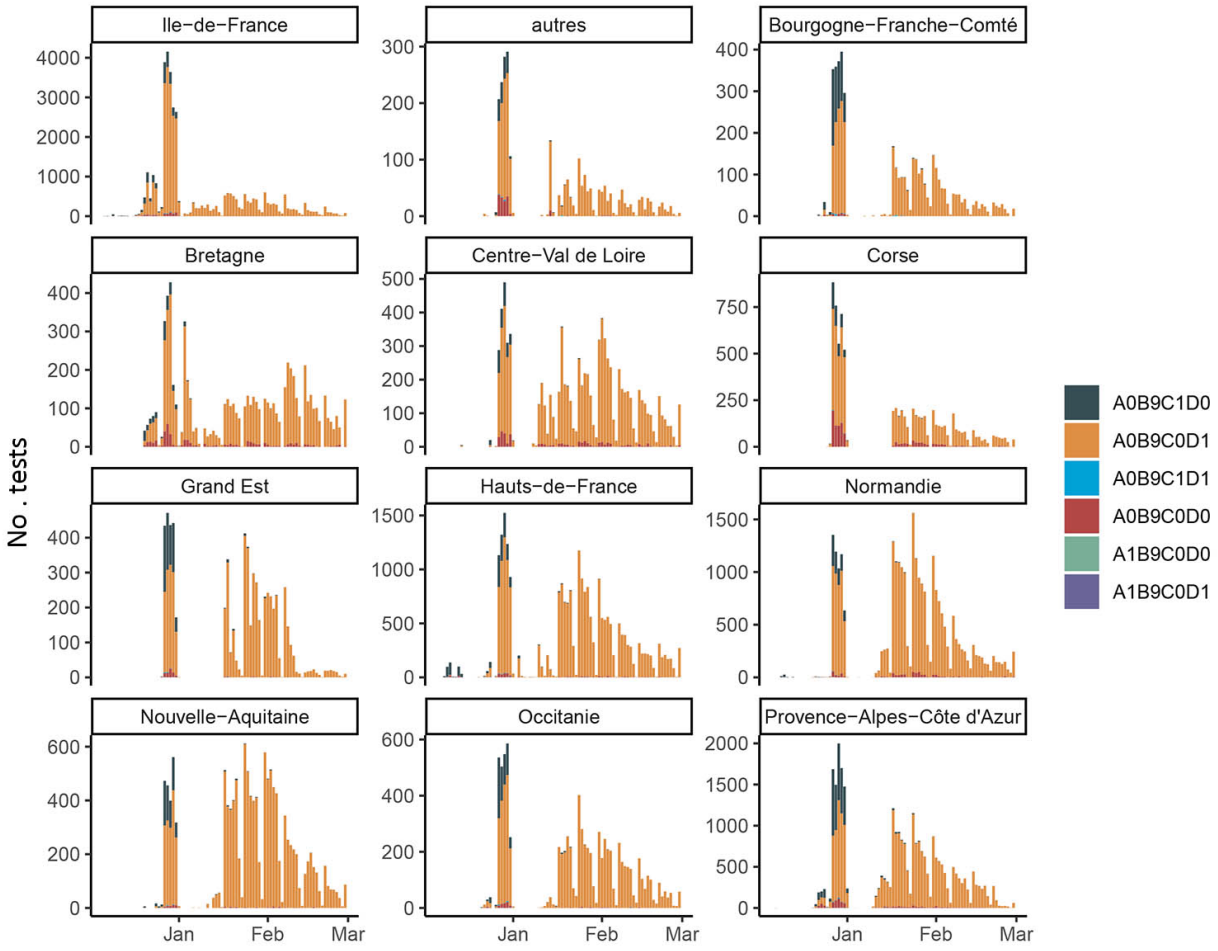

Appendix 1 Figure 2. Variant-specific screening test incidence data per French region for the ID solutions Revolution test. The color indicates the test result. Regions with too few tests are pooled in the "other" category.

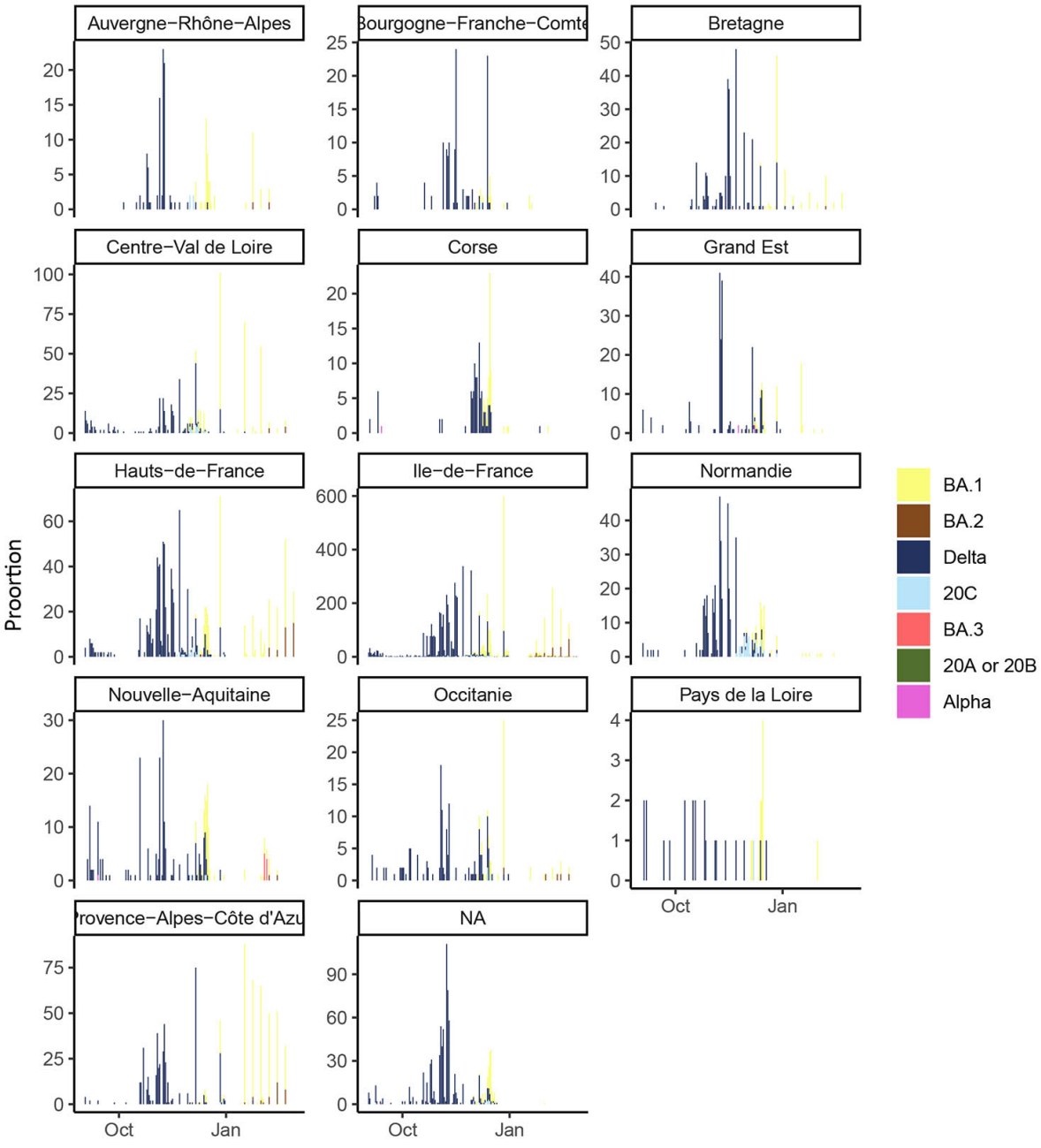

Appendix 1 Figure 3. Lineage-specific incidence data per French region using whole genome sequencing. Samples with missing regions are in the “NA” category.

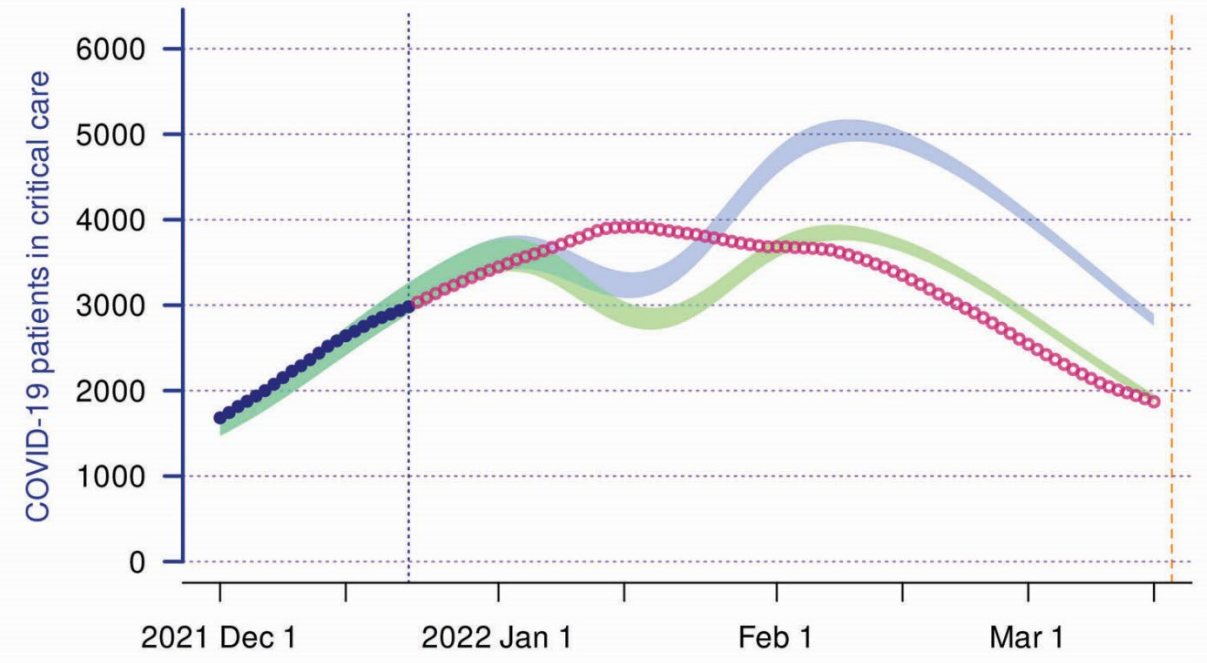

Appendix 1 Figure 4. Epidemiologic modeling of scenarios for French national critical care unit (CCU) occupancy from December 2021 to Mid-March 22 with different Omicron virulence and immune evasion properties. The vertical blue line indicates the day the simulations were performed (22 Dec 2021), using solely epidemiologic, hospital, and virological data available to that date. In particular, the dark blue dots indicate the nationwide number critical care beds occupied by COVID-19 patients included for the model inference. The yellow vertical bar shows the date the figure was made. The red circles correspond to the data observed after the computation of the projections (data from Santé publique France). The shaded envelope the 95% range of the optimistic (green) and pessimistic (blue) scenarios according to the estimates available on Dec 22 2021. As expected, the model captures the CCU dynamics during the first 2 weeks. The underestimation of the CCU occupancy in mid-Jan is related to the (overoptimistic) assumption that the Delta epidemic was under control when the model was made. This led to a merging between the Delta and the Omicron/BA.1 epidemic peaks in CCU on January 24, 2022. The 'optimistic' scenario (with low Omicron virulence and high vaccine protection) provided an accurate lower boundary for CCU occupancy until the end of January 2022. See the main text and the supplementary methods for more details about the model and its assumptions.